Available online at www.sciencedirect.com

ScienceDirect

Physics Procedia 56 (2014) 535 – 544

Physics Procedia

8th International Conference on Photonic Technologies LANE 2014

Remote Laser Welding of zinc coated steel sheets in an edge lap configuration with zero gap

Christian Roos[a,]*, Michael Schmidt[b,c]

[a] *BMW Group, Forschungs- und Innovationszentrum, Knorrstraße 147; 80788 München*

[b] *Institute of Photonic Technologies (LPT), Friedrich-Alexander-Universität Erlangen-Nürnberg, Konrad-Zuse-Str. 3-5, 91052 Erlangen, Germany*

[c] *Erlangen Graduate School in Advanced Optical Technologies (SAOT), Friedrich-Alexander-Universität Erlangen-Nürnberg, Paul-Gordan-Str. 6, 91052 Erlangen, Germany*

Abstract

Remote Laser Welding (RLW) of zinc-coated steel sheets is a great challenge for the automotive industry but offers high potentials with respect to flexibility and costs. In state of the art applications, sheets are joined in overlap configuration with a preset gap for a stable zinc degassing. This paper investigates RLW of fillets without a preset gap and conditions for a stable process. The influence of process parameters on weld quality and process stability is shown. Experimental data give evidence, that the degassing of zinc through the capillary and the rear melt pool are the major degassing mechanisms. Furthermore the paper gives experimental validation of the zinc degassing in advance of the process zone to the open side of the fillet. Chemical analysis of the hot-dip galvanized zinc coating proof the iron-zinc-alloys to be the reason for a limited effectiveness of this mechanism in comparison to pure zinc as intermediate.

Peer-review under responsibility of the Bayerisches Laserzentrum GmbH

Keywords: Remote laser welding; fillet welds; zero gap; zinc transport mechanisms

1. Introduction

Remote laser welding is an appealing joining technique for the automotive industry. To prevent corrosion damage of the car body, mainly zinc coated steel sheets are used. Due to the relatively low boiling temperature of zinc in comparison to steel, the degassing zinc vapor disturbs the process zone and leads to spattering and seam

* Corresponding author. Tel.: +49-89-382-24784 .
E-mail address: christian.roos@bmw.de

Peer-review under responsibility of the Bayerisches Laserzentrum GmbH
doi:10.1016/j.phpro.2014.08.025

imperfections. Understanding the zinc degassing mechanisms is therefore crucial for implementing stable industrial welding processes. In state of the art remote laser welding applications a preset gap between the joining partners is used to stabilize the zinc degassing through the capillary. This additional process step causes additional costs, process time and problems with respect to reproducibility. Thus alternative joining methods for joining zinc coated steel sheets are demanded.

[GRUPP 2003] and [PIETERS 2006] give experimental evidence, that welding in edge lap configuration without a preset gap allows stable welding processes. A complete experimental study about the major influencing process parameters, their impact on the weld seam quality and the borders of a stable process is not yet given. Also in sense of an analytical model, many investigations analyze the zinc degassing in overlap configuration, whereas only little is known about such mechanisms for fillet joints. Hence this paper presents an experimental study and analytical relations for the zinc transport mechanisms for welding in edge lap configuration. The influence of the major process parameters on the weld seam quality and the borders for a stable process are experimentally investigated and a model for the underlying principles is presented.

1.1. Fundamentals

In case of welding in overlap configuration different investigations give models about the zinc degassing mechanisms through the process zone. [KAEGELER 2009] distinguishes between the zinc degassing through the capillary and through the rear melt pool. Experimental studies and simulations show, that a preset gap of more than 50 µm leads to a stable aperture in the front melt film of the capillary and results in a stabile zinc vapor flow through the capillary apertures. If there is no gap, the pressure of the zinc in front of the capillary increases until it expands explosively. This disturbs the melt flow and results in spattering and seam imperfections.

[FABBRO 2006] proposes a different model, where he describes the zinc vapor as a high pressure jet, which penetrates through the front capillary wall. Probable disturbances in the melt pool, which result from the collision of the zinc jet with the rear capillary wall, can be reduced by using such process parameters, that the zinc jet points downward and degasses through the lower capillary aperture. This model is supported by [PAN 2010], who gives experimental evidence, that thicker zinc coatings of 20 µm lead to a higher pressure of this zinc jet, hence to a more constant degassing through the enlarged capillary.

A second zinc degassing mechanism through the process zone is described in [KAEGELER 2009, PAN 2012]. Due to the characteristics of the isotherms, additional zinc vaporizes besides the melt pool. If no gap is present the zinc vapor expands and degasses through an explosion in the rear part of the melt pool, which results in large spatters, and blowout holes.

An experimental validation for the presence of these two distinct zinc degassing mechanisms is given in [HESSE 2008], where the zinc on certain areas of the specimen was removed. By using high speed video analysis it was shown, that the process dynamics of welding zinc coated steel sheets in overlap configuration with zero gap results from a superposition of the two distinct mechanisms described above.

Only few investigations were conducted on laser welding of zinc coated steel in edge lap configuration. [GRUPP 2003] proposes the beam positioning relative to the edge and the lateral beam inclination as the major process parameters for welding fillets. In case of uncoated steel sheets acceptable weld seams are achieved with a beam positioning in a range of about 0.5 mm dependent on the lateral angle. Later studies conducted by [PIETERS 2006] give spattering as predominant problem, which can be avoided only at low welding speeds. Analysis of cross section showed zinc accumulations next to the weld seam on the lower sheet. From that fact it was concluded, that the zinc vapor in front of the process zone evaporates to the free side of the edge lap and pushes the liquid melt outside, so it cannot influence the process zone. Since no further experimental proof for this assumption is presented and this additional mechanism does not explain the described spattering, further investigations are necessary.

1.2. Experimental setup

For the conducted experiments a Yb:YAG-fibre-laser source with a maximum output power of 6 kW is used. The beam is positioned with a scanner and results in a focus diameter of 640 µm and a focal distance of 472 mm. The

fixture is specially designed for welding fillets and allows a position accuracy of ± 20 µm. The clamps are actuated pneumatically and press the sheets with a force of 300 N to achieve a zero gap. An additional air stream directly above the top sheet reduces the interaction between metal vapor and laser beam and deflects the emitted spatters from the optic head. The metal sheets used for the experiments have a thickness of d_B = 0.8 mm and are hot-dip galvanized DX54 with a coating thickness of 7 and 20 µm and uncoated DC04. The effect of pure zinc on the welding process is studied by using zinc foil consisting of 99.99 % pure zinc with a thickness of 25 and 70 µm as an intermediate between the uncoated sheets.

2. Experimental analysis of the process parameters

2.1. Effect of beam positioning and inclination

The positioning and the lateral inclination angle of the laser beam relative to the work piece are the major influencing factors on weld seam geometry (see Fig. 1). As shown in Fig. 1(left) the beam positioning y_{off} perpendicular to the welding direction governs the achieved joining width and the seam profile. If the beam is positioned more to the lower sheet (y_{off} < 0 mm) the process results in an insufficient joining width and full penetration. With increasing y_{off} the joining width increases, the penetration depth decreases and a spherical seam profile is provoked. As shown in Fig. 1(right) the lateral inclination of the laser beam affects the seam geometry and the width of the heat affected zone. A larger lateral angle leads to reduced process sensitivity to variable beam positioning. Full penetration was reached between 10 and 65° and the joining width increased with larger angles.

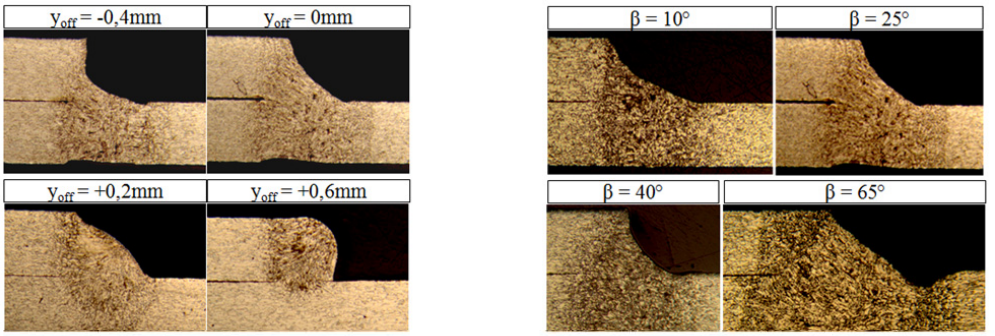

Fig. 1. Effect of beam positioning y_{off} (left) and lateral beam inclination β (right) on the weld seam geometry. (P_L = 1.45 kW, v_s = 3 m/min, β(left) = 25°, y_{off}(right) = 0 mm, D_f = 640 µm, d_B = 0.8mm DX54).

The quantitative influence of beam positioning and inclination on the tensile shear breaking force and the surface quality of the resulting weld seam are shown in Fig. 2. A maximum shear break force is reached for $0 \leq y_{off} \leq +0.4$ mm, where a larger lateral angle achieved better results with positioning on the lower sheet. In contrast to the shear force, a decrease of seam quality is observed with increasing lateral inclination. Moreover, higher y_{off} lead to low seam quality and larger deviation. It is obvious that $y_{off} > +0.4$ mm represents the transition to the overlap configuration. This effect is amplified by an increased lateral inclination angle of the laser beam. Welds with a percentage of good seam surface above 80% could only be realized with angles of $\beta < 40°$ and $y_{off} < +0.4$ mm.

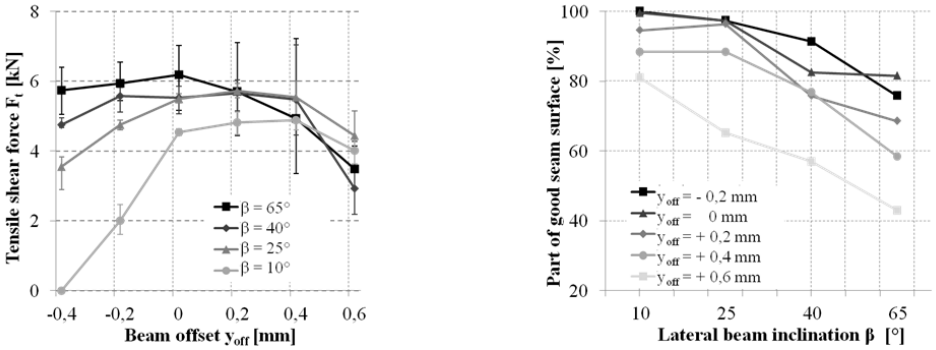

Fig. 2. Effect of beam positioning y_{off} and inclination β on tensile shear breaking force (left) and seam surface quality (right). (P_L = 1.45 kW, v_s = 3 m/min, D_f = 640 µm, d_B = 0.8mm DX54Z100, L_{seam} = 30 mm).

2.2. Effect of welding speed and degree of penetration

The effect of welding speed and degree of penetration is shown in Fig. 3. The energy per unit length E_u was kept constant by adapting the laser power proportionally to the welding speed. In order to obtain different degrees of penetration the thickness of the bottom sheet was changed from 0.8 to 2 mm while keeping E_u constant. For full penetration welding the welding speed has only little impact on the tensile shear breaking force and almost none on the surface quality. In case of welding without weld root penetration, the quality of the seam surface decreases massively and no good welds could be produced above 3 m/min.

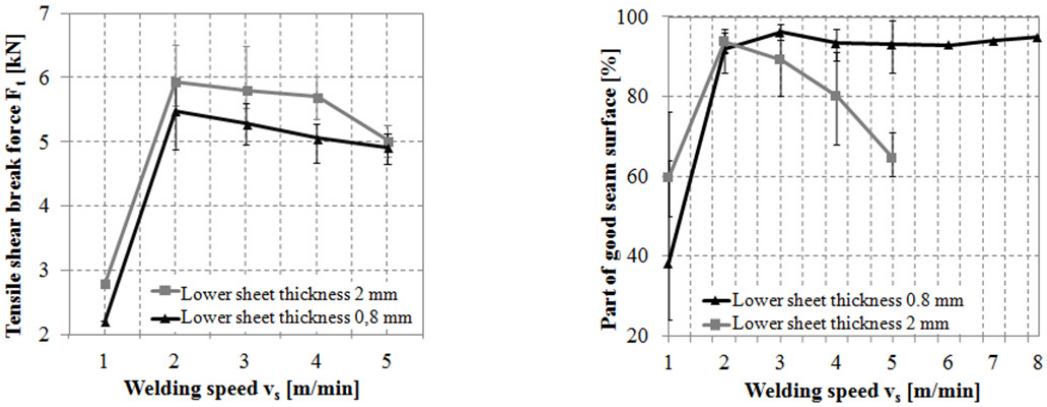

Fig. 3. Effect of welding speed and degree of penetration on tensile shear breaking force (left) and surface quality (right) (E_u = 29 J/mm, y_{off} = 0 mm, D_f = 640 µm, β = 25°, d_B = 0.8mm DX54Z100, L_{seam} = 30 mm).

3. Interpretation and experimental validation

Based on the experimental data, interpretations are derived and experimentally validated in order to explain the underlying principles and identified process borders. First the applied model is presented and afterwards the distinct zinc transport mechanisms are separately investigated in detail.

3.1. Zinc transport mechanisms for fillet welds

The state of the art gives an understanding of the zinc transport mechanisms through the capillary and the rear melt pool in case of welding in overlap configuration. These models are now applied and their validity is checked

for the geometry of a fillet weld. The zinc degassing in advance of the process zone is only mentioned as a rough hypothesis in [PIETERS 2008] and should therefore be analyzed and validated in detail in the following chapter.

The following experimental validation is based on three major zinc transport mechanisms, which are schematically presented in Fig. 4. The degassing of zinc vapor in advance of the process zone is enabled by the geometry of the fillet. The zinc between the sheets is vaporized in front of the front capillary melt film and degasses through the free side of the fillet. If no complete degassing takes place, the vapor expands explosively into the capillary and leads to melt pool instabilities and spattering. The additionally generated zinc vapor beside the melt pool leads to melt ejections in the rear part of the melt pool.

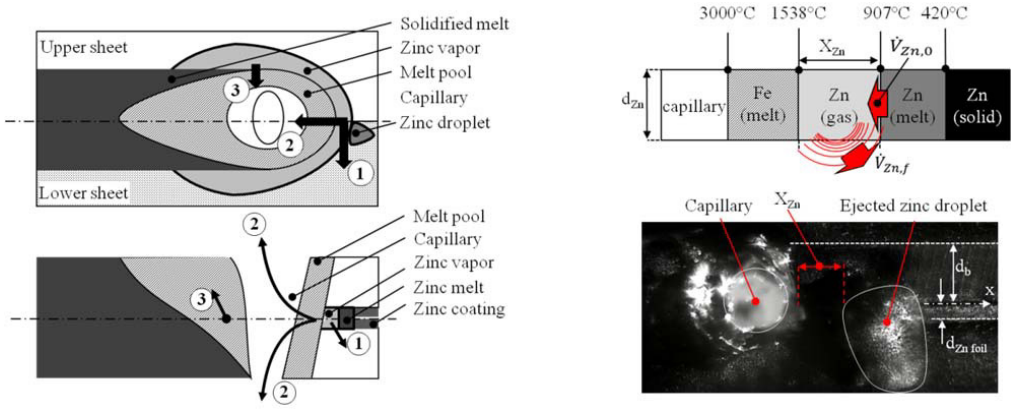

Fig. 4. Zinc degassing mechanisms in edge lap configuration with zero gap (left): Degassing in advance of the process zone (1), through the capillary (2) and through the rear melt pool (3). Schematic structure of the different aggregates inside the zinc coating layer in advance of the process zone (right). Experimental proof for the existence of mechanism (3) by welding uncoated steel sheets with 25 µm zinc foil as intermediate: Formation of zinc droplets ahead of the process zone (right).

3.2. Zinc degassing in advance of the process zone

The zinc coated area between the sheets is assumed to have a structure as presented in Fig. 4 (right), consisting of a zinc vapor chamber, which is separated from the capillary by a molten film of the capillary front. The advantage of this degassing mechanism is that it does not influence the melt pool dynamics and does therefore not reduce the process stability. Ideally the complete produced zinc vapor flow $\dot{V}_{Zn,0}$ degasses through the free side of the fillet $\dot{V}_{Zn,f}$, so that the vapor flow inside the capillary $\dot{V}_{Zn,c} = \dot{V}_{Zn,0} - \dot{V}_{Zn,f}$ equals zero. The existence of this mechanism can be seen on high speed video images in Fig. 4 (right): 25 µm zinc foil was placed between uncoated steel sheets and during welding the zinc vapor in advance of the process zone expands and pushes out the zinc melt ahead in regular time intervals. This leads to molten zinc droplets, which are shown exemplarily in Fig. 4. As it can be seen on the high speed images, a defined distance X_{Zn} lies between the capillary front and the melt expulsion of zinc melt. Increasing the welding speed resulted in a decreasing X_{Zn}. For welding speeds of above 5 m/min the seam showed minor imperfections and few spatters were emitted during the process. In case of higher welding speeds, a stable gap between the sheets is visible on the inner side of the capillary (see Fig. 5 left). From this gap a zinc jet is emitted, which pushes back the rear melt pool, emits spatters from it and enlarges the capillary. Since for lower welding speeds no such gap is present and smooth seam surfaces are provided, it can be assumed, that all vaporized zinc evaporates ahead of the process zone.

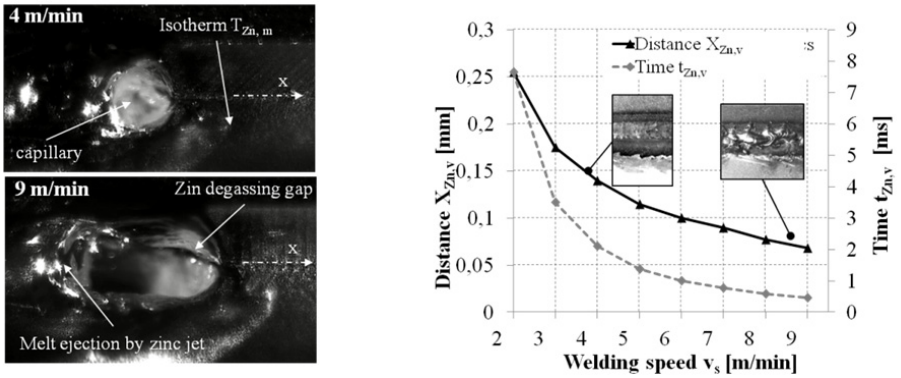

Fig. 5. High speed video images of zinc degassing in advance of the process zone in dependency of the welding speed (left). Analytical determined values for the distance $X_{Zn,v}$ and the resulting available time for zinc degassing in advance $t_{Zn,v}$ (right).
(P_L = 1.45 kW, y_{off} = 0 mm, β = 25°, D_f = 640 µm, d_B = 0.8mm, DC04 with 25 µm zinc foil).

In order to get a deeper understanding of the limitations of this mechanism, a heat conduction model is applied to calculate X_{Zn} analytically (see Fig. 5 right). The capillary was approximated by a cylindrical heat source with the iron boiling temperature as a boundary condition. The cylinder diameter was assumed to be equal to the beam diameter and independent of the process parameters. The isotherms follow equation (1) [LANKALAPALLI 2006]:

$$T(r,\theta) = T_V - (T_V - T_0)\left[1 - exp(-Pe \cdot r^* cos\theta) \sum_{n=0}^{\infty} \epsilon_n \frac{I_n(Pe)}{K_n(Pe)} K_n(Pe \cdot r^*) cos(n\theta)\right] \quad (1)$$

Additionally Fig. 5 shows the available time $t_{Zn,v} = X_{Zn} / v_s$ for the zinc to completely degas in advance of the front melt film. With increasing welding speed $t_{Zn,v}$ decreases and no complete degassing ahead takes place. Thus a gap in the inner side of the capillary is formed, through which the zinc jet enters the capillary and leads to minor disturbances and spatters. The gap and the resulting zinc degassing are stable and therefore the resulting seams show almost no imperfections in its surface.

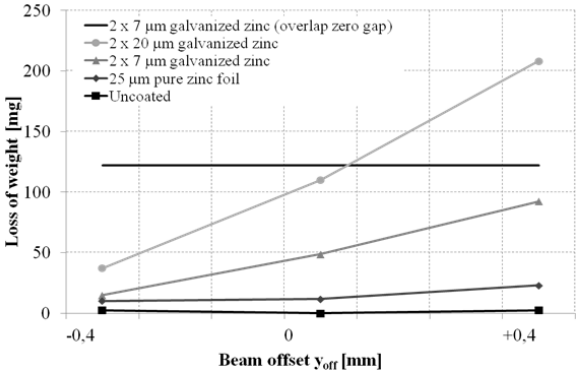

Fig. 6. Loss of weight due to spattering for hot-dip galvanized zinc coatings with 7 and 20 µm thickness, uncoated steel sheets and uncoated sheets with 25 µm zinc foil as an intermediate. (P_L = 1.45 kW, v_s = 3 m/min, β = 25°, D_f = 640 µm, d_B = 0.8mm, L_{seam} = 30 mm).

The process behavior of hot-dip galvanized coating was found to be significantly different from that of pure zinc. Fig. 6 shows the loss of weight due to spatters in dependency of the beam offset y_{off}. As it can be seen, the specimen with zinc foil as intermediate metal show almost no loss of weight and shows similar results as uncoated steel

sheets. In contrast to that, the galvanized coatings show strong spattering and insufficient seam quality. A beam positioning to the upper sheet does in general lead to an increased amount of spatters and a reduced seam surface quality (see Fig. 2). In order to compare fillets with overlap welds with zero gap Fig. 6 gives the loss of weight for an overlap weld with P_L = 2 kW. At a beam positioning of y_{off} = 0 mm the fillet achieves 80 % less spatters than the overlap weld with zero gap.

This significant difference between zinc foil and hot-dip galvanized coating results from its chemical properties, which are shown in a GDOES analysis in Fig. 7 (left). The percentage of zinc lies above 95% only until a coating depth of 5 µm. Afterwards the zinc percentage decreases slowly until it reaches 5% at a depth of about 12 µm. [REUMONT 2000] present an overview of the resulting zinc-iron-alloys in-between and their specific melting temperature in a phase diagram (see Fig. 7 right). In accordance to the iron percentage the melting temperature increases. Since the melting temperature correlates with the boiling temperature of every compound, it is obvious, that the degassing ahead does not work for galvanized coatings due to the significantly higher boiling temperature. Every depth in the galvanized coating represents a specific iron-zinc-alloy in the phase diagram. These compounds are generated during the galvanization process, owing to diffusion effects, which can be reduced by adding aluminium during the galvanization. The resulting iron-aluminium compounds will also have high boiling temperatures, but might have smaller thicknesses, hence result in less disturbances of the process [REUMONT 2000]. The significantly higher vaporization temperature of hot-dip galvanized zinc coating compared with pure zinc is not yet included in many models, but has a strong impact on the process behaviour. As it can be seen from Fig. 7 some alloys do melt and vaporize directly in front of the molten front capillary wall and do therefore lead to disturbances in the process.

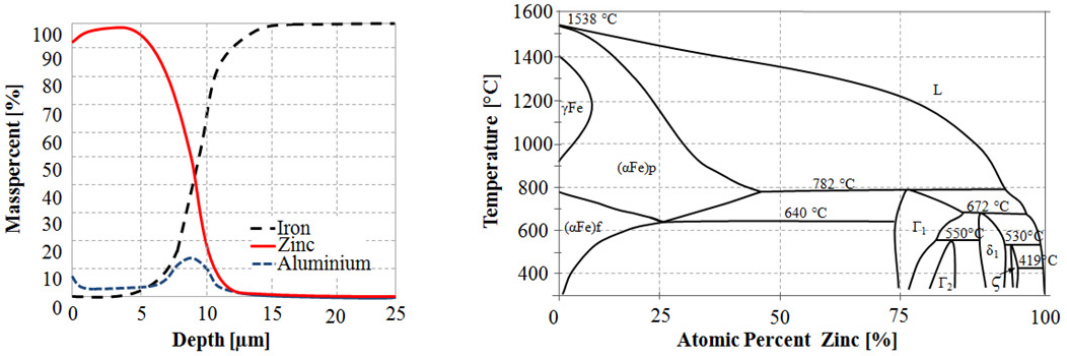

Fig. 7. GDOES analysis of galvanized zinc coating with 7 µm thickness for the elements iron, zinc and aluminium (scaled with factor 20 for better presentation) (left). Iron-zinc-phase diagram [REUMONT 2000] (right).

From the presented experimental results, one can conclude, that degassing in advance of the process zone is no major degassing mechanism for hot-dip galvanized coatings. Due to the significantly higher melting and vaporization temperatures of the zinc-iron-alloys, X_{Zn} and $t_{Zn,v}$ decreases massively, so that the zinc vapor is forced to predominantly degas explosively through the process zone.

3.3. Zinc degassing through the process zone

Zinc degassing through the process zone occurs, if zinc-iron-alloys are present, as it is the case for hot-dip galvanized coatings. [KAEGELER 2009] states, that the degassing through the capillary leads to rather small spatters around the capillary apertures, whereas the degassing through the rear melt pool leads rather to big melt ejections. This is supported by [PAN 2011], who concludes from high speed video images, that blow holes do result from the additional zinc vaporization behind the capillary. Furthermore he states, that this effect is reduced in case of thicker coatings (20 µm), because the capillary is more elongated and stable and therefore allows a bigger amount of zinc to degas through the capillary. Quantitative investigations on this effect have not yet been conducted and in case of edge lap configuration no such experiments were presented so far.

As it is shown in Fig. 8, it is assumed, that the intensity of the explosive degassing beside the melt pool increases with the width ΔB_{Zn} of the area of additional zinc evaporation, since more zinc needs to degas. The distance ΔL_{Zn} between the capillary and the largest width of the zinc evaporation isotherm determines, if the disturbances lead to imperfections in the resulting weld seam. If disturbances are closer at the solidifying end of the melt pool, little time is available to compensate the occurring turbulences in the melt flow. Increasing ΔL_{Zn} therefore results in a higher the probability for surface imperfections.

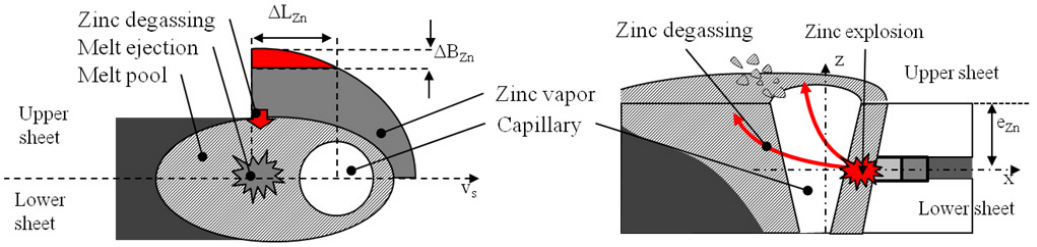

Fig. 8. Zinc degassing mechanisms through the process zone: additional zinc vapour degassing beside the rear melt pool (left); Degassing through the front melt film into the capillary (right).

In case of degassing through the capillary (Fig. 8 right), e_{Zn} describes the length from the root of zinc vaporization to the capillary aperture and determines the amount of emitted spatters and the grade of instability caused by this mechanism. In case of fillet welding, e_{Zn} increases with a beam positioning on the upper sheet and reaches its maximum at the transition to overlap welding at $y_{off} > +0.4$ mm (see Fig. 1).
In order to achieve quantitative data about the effectiveness of these distinct mechanisms, a similar setup to [HESSE 2008] is used (see Fig. 9). For the specimen the 20 µm thick zinc coating was removed at specific areas by means of laser ablation: one kind was produced with only a 0.5 mm wide zinc coating stripe with its middle line at $y_{off} = +0.25$ mm and another, where only this same stripe was removed. This preparation allowed analyzing the effects separated from each other.

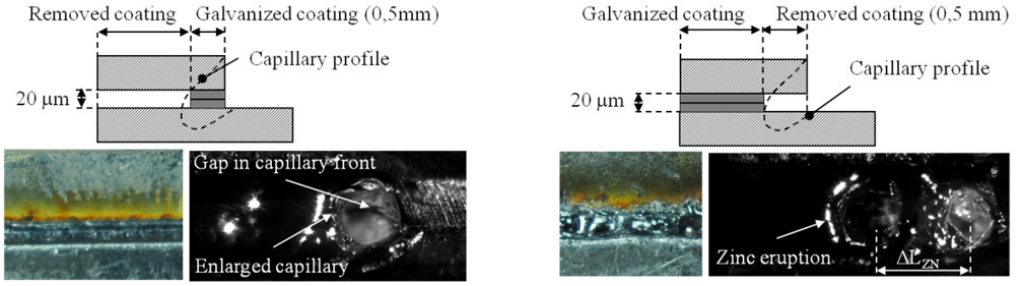

Fig. 9. Experimental setup for analyzing the zinc degassing mechanisms through the process zone: zinc coating removal besides the capillary width (left) and on the capillary width (right). ($P_L = 2{,}5$ kW, $v_s = 5$ m/min, $y_{off} = +0.2$ mm, $\beta = 25°$, $D_f = 640$ µm, $d_B = 0.8$mm).

High speed video images of these experiments and the resulting seams are exemplarily shown in Fig. 9 and do confirm the assumed mechanisms for welding in edge lap configuration. Fig. 9 (left) shows a stable melt pool and capillary for the degassing through the capillary and the resulting seam with a very smooth surface. The capillary shows a small gap on its front wall, where the zinc jet degasses and leads to little spattering at the capillary aperture.
In contrast to that, Fig. 9 (right) shows an insufficient weld seam quality resulting from the zinc degassing beside the rear melt pool. In regular time intervals an eruption occurs in constant distance behind the capillary and leads to disturbances of the melt pool. The remaining voids after the ejection cannot be filled with molten material owing to the increasing viscosity of the already cold melt pool and to the reduced time before solidification. Therefore holes and pores remain in the seam and a poor seam quality results.

The underlying principles for the emission of spatters due to the degassing through the capillary are described in [WEBERPALS 2011]. For welding in edge lap configuration, the beam offset y_{off} becomes a main influencing factor on the amount of spatters. As shown in Fig. 8 (right) the length e_{Zn} increases with the beam offset to the upper sheet. With increasing y_{off} the zinc jet will cause more disturbances, because it impinges more on the center of the rear melt pool, where then more melt is ejected and spatters are accelerated over a longer time.

Fig. 10 gives a more detailed understanding of the degassing trough the rear melt pool. Based on equation (1) ΔL_{Zn} and ΔB_{Zn} were calculated in dependency of the welding speed and compared with experimental values from high speed video images. From the three exemplary images one can see, that an increasing welding speed leads to a larger distance between the eruption and the capillary. For welding speeds below 3 m/min, the zinc beside the melt pool degasses into the capillary and leads to complete destabilization of the capillary. The analytical determined values for ΔL_{Zn} show similar characteristics. It is interesting to note that the additional vaporized zinc beside the melt pool ΔB_{Zn} declines with increasing welding speed. Low welding speeds do therefore lead to bigger eruptions but those do not cause necessarily insufficient weld quality, because defects can be annihilated in the stable rear melt pool.

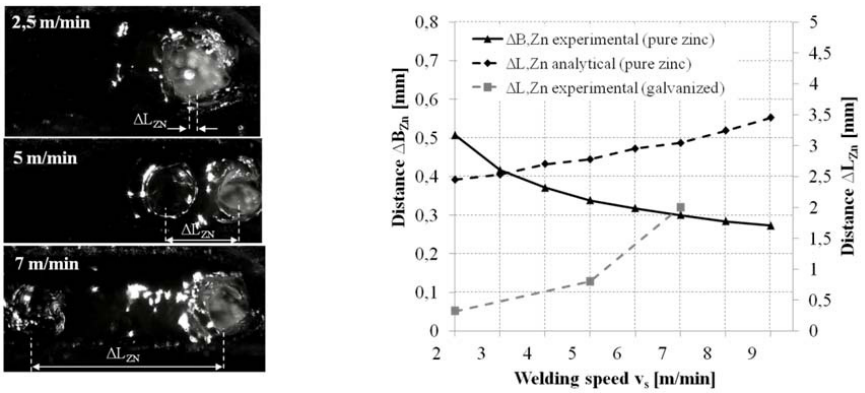

Fig. 10. High speed video images of the eruptions in the rear melt pool for different welding velocities (left). Calculation of ΔB_{Zn} and L_{Zn} for pure zinc as intermediate and comparison with L_{Zn} for galvanized coatings (right). (E = 29 J /mm, y_{off} = + 0.2 mm, β = 25°, D_f = 640 µm, d_B = 0.8mm).

Fig. 11 gives experimental data about the described relations and quantifies the relative influence of the two degassing mechanisms on the weld quality based on the experimental setup described in Fig. 9.

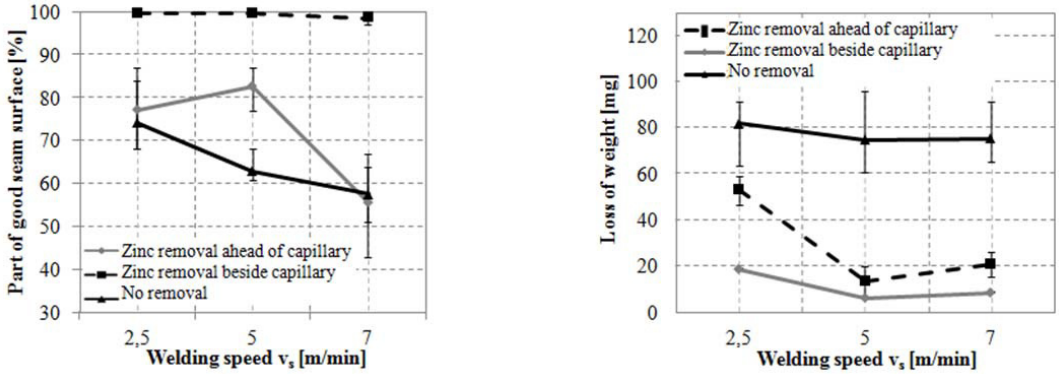

Fig. 11. Superposition of the distinct zinc transport mechanisms through the process zone and its effect on seam surface quality (left) and loss of weight due to spatters (right). (E = 29 J/mm, y_{off} = + 0.2 mm, β = 25°, D_f = 640 µm, d_B = 0.8mm, L_{seam} = 30 mm).

It can be seen, that the degassing through the capillary leads to only few spatters (< 20 mg on 25 mm length) and to very good seam surfaces. In contrast to that the degassing through the rear melt pool leads to three times more spatters and insufficient seam qualities. Still the quality is found to be better compared to the reference seam with a

complete 20 µm coating. The amount of spatters has its maximum at low welding speeds, when the eruptions occur at low ΔL_{Zn}. At these positions the effect is amplified by the metal vapor dynamics in the capillary.

4. Summary and conclusion

The paper presented an experimental investigation on the influencing process parameters in remote laser welding of fillet joints and identified the process window for a stable welding process. It offers a new understanding of the underlying mechanisms, which determine the limits for a stable welding process. The zinc degassing in advance of the capillary was found not to be a dominant mechanism in case of welding steel sheets with hot-dip galvanized coatings. The diffusion processes during galvanization lead to iron-zinc-alloys with much higher boiling temperatures compared to pure zinc and therefore parts of the coating do vaporize directly at the capillary instead of degassing well in advance. Though, in case of pure zinc foil as an intermediate the mechanism was shown to be very effective.

It was shown, that the beam positioning directly influences the amount of emitted spatters from the capillary and the strength of the resulting joint. The positioning tolerance to achieve seams with good strength and few spatters is $y_{off} = \pm 0.2$ mm. The influence of the welding speed on the seam quality was explained by the mechanism of zinc degassing through the rear melt pool. Experimental evidence was presented, that this mechanism is responsible for insufficient seam quality at higher welding speeds above 3 m/min. Analytics explained this relation with the increasing distance ΔL_{Zn} between the maximum width of the zinc vapor area and the capillary. The strong spattering at low welding speeds was shown to result from the additional vaporized zinc beside the capillary ΔB_{Zn}, which has its maximum at lower welding speeds.

With the presented results a stable remote laser welding process for fillets with zero gap is achieved. To make use of its potentials in industrial applications, the rather high demands with respect to beam positioning relative to the edge afford new technical solutions for seam tracking for scanner technology. A new approach for industrial implementation of the process is presented in [OEFELE & ROOS 2014].

Acknowledgements

The presented experiments in this paper were conducted at the Research and Innovation Centre of BMW Group and the developed research work was supported by the Institute of Photonic Technologies. Additional gratitude belongs to H. Langrieger, A. Kaipf and A. Bachmann, who took part in this work during their final theses.

References

E. Beyer, 1995. Schweißen mit Laser. Grundlagen. Berlin 1995: Springer-Verlag. ISBN: 3-540-52674-9.

R. Fabbro; F. Coste; D. Goebels; M. Kielwasser, 2006. Study of CW Nd-Yag laser welding of Zn-coated steel sheets. Journal of applied Physics D: Applied Physics 39 (2006).

M. Grupp; T. Seefeld; F. Vollertsen, 2003. Laser Beam Welding with Scanner. Proceedings of the Second International WLT-Conference on Lasers in Manufacturing 2003, Munich. BIAS – Bremer Institut für angewandte Strahltechnik: Juni 2003.

T. Hesse, 2008. Neue Erkenntnisse und Lösungsgrundlagen beim Laserstrahl-schweißen von verzinkten Stahlblechen. TRUMPF GmbH + Co. KG. In: EALA 2008.

C. Kaegeler; A. Grimm; A. Otto; M. Schmidt, 2009. Frequency-modulated zero-gap laser beam welding of zinc-coated steel sheets in an overlap joint configuration. Proceedings of the Fifth International WLT-Conference on Lasers in Manufacturing. München: Juni 2009.

K. N. Lankalapalli; J. F. Tu; M. Gartner, 1996. A model for estimating penetration depth of laser welding processes. J. Phys. D: Appl. Phys. 29 (1996).

F. Oefele; C. Roos, 2014. Remote laser beam welding with inline seam tracking. BMW Group. In: EALA 2014.

Y. Pan, 2008. Laser Welding of Zinc Coated Steel without a Pre-set Gap. Dissertation TU Delft (2011). ISBN 978-90-77172-643.

Y. Pan; I. M. Richardson, 2008. Effect of zinc coating thickness in gap-free laser welding of galvanized sheet steels. Paper 607. In: 3rd Pacific International Conference on Application of Lasers and Optics (2008).

R. Pieters; J. Bakels; M. Hermans; G. den Ouden, 2006. Laser welding of zinc coated steels in an edge lap configuration. Journal of laser applications. Volume 18, Number 3: August 2006.

G. Reumont; P. Perrot; J. M. Fiorani; J. Hertz, 2000. Thermodynamic Assessment of the Fe-Zn System. Basic and Applied Research: Section I. Journal of Phase Equilibria Vol. 21 No.4: August 2000.

J.-P. Weberpals, 2010. Nutzen und Grenzen guter Fokussierbarkeit beim Laser-schweißen. Laser in der Materialbearbeitung, Forschungsberichte des IFSW. Esslingen: Herbert Utz Verlag 2010.